Control of Contact Forces: the Role of Tactile Feedback for Contact Localization

Andrea Del Prete, Francesco Nori, Giorgio Metta, Lorenzo Natale

***Abstract*— This paper investigates the role of precise estimation of contact points in force control. This analysis is motivated by scenarios in which robots make contacts, either voluntarily or accidentally, with different parts of their body. Control paradigms that are usually implemented in robots with no tactile system, make the hypothesis that contacts occur at the end-effectors only. In this paper we try to investigate what happens when this assumption is not verified. First we consider a simple feedforward force control law, and then we extend it by introducing a proportional feedback term. For both controllers we find the error in the resulting contact force, that is induced by a hypothetic error in the estimation of the contact point. We show that, depending on the geometry of the contact, incorrect estimation of contact points can induce undesired joint accelerations. We validate the presented analysis with tests on a simulated robot arm. Moreover we consider a complex real world scenario, where most of the assumptions that we make in our analytical derivation do not hold. Through tests on the iCub humanoid robot we see how errors in contact localization affect the performance of a parallel force/position controller. In order to estimate contact points and contact forces on the forearm of the iCub we do not use any model of the environment, but we exploit its 6-axis force/torque sensor and its sensorized skin.**

I. Introduction

After decades of research in robotics, robots are still a long way off being able to operate in human environments. The inability to deal with uncertainties in the geometry of the environment is maybe the major limitation that prevents robots from safely interacting with humans.

Research has tried to tackle this problem at the control level. Traditional stiff position control tries to follow a desired position trajectory considering external forces as disturbances, hence large contact forces may be exerted, leading to instability or physical damage. Controlling the interaction forces has been shown to be a powerful technique to overcome these limitations. In the literature we can find different approaches to force control: explicit force control, impedance/admittance control [1], hybrid control [2], hybrid impedance control [3], parallel control [4].

Nevertheless, most of these works have only focused on controlling forces that are exerted at the end-effectors, namely the hands for manipulation tasks and the feet for walking. Restricting contacts to end-effectors is a quite strong assumption, since i) uncertainties in the environment may result in unplanned contacts at other body parts, and ii) contacts at other body parts may be necessary to perform certain tasks. If you are reading this paper, for instance, you are likely to be making contact with the environment with at least four points that are not end-effectors: bottom and back against the chair, and elbows on the desk.

Some works do not make any assumption about the contact location, trying to control the joint torques rather than the contact forces. This approach ensures bounded contact forces, but do not allow a real contact force control. Various theoretical frameworks for modeling and control of robots that are subject to multiple contacts have been proposed [5], [6], [7], but they have not gone beyond end-effector contacts when tested on real platforms.

What has really prevented contact force control from spreading in robotics is the lack of robust contact force measurements, that is the ability to measure multiple contact forces and their locations on the robot's body. Gordon et al.[8] have verified that it is not possible to obtain high-resolution contact-position measurements from only joint torque sensing. In this scenario a tactile system becomes paramount.

Despite these difficulties, in the literature we can find some examples of contact force control. In [9], Park et al. presented the first implementation of multi-link multi-contact force control, with demonstration on a 6-DOF PUMA560 manipulator. The robot was able to control three contact forces, distributed on its end-effector and third link, while motion was controlled in the remaining three DOFs through null space control. Due to the limited sensing capabilities of the test platform, the measure of contact forces and contact locations required i) an external force sensor mounted on one of the contact points and ii) geometric models of both robot and environment. Relying on geometric models is risky because modeling uncertainties may cause the controller to perform inconsistently in response to small errors.

In [10], the authors describe a model predictive controller (MPC) that allows a robot arm to reach with its end-effector, while regulating contact forces across its entire surface. This work exploits tactile sensing, it does not use a model of the environment and it handles contacts at unpredictable locations.

Motivated by works such as [9] and [10], in this paper we evaluate analytically the impact of errors in the contact point estimation on the performance of contact force control. Even though the effect that errors in the estimation of contact location have on contact force control is not surprising, to the best of our knowledge this is the first analytical analysis of their relationship. First, in section II-A, we consider a simple

The authors are with the Robotics, Brain and Cognitive Sciences Department, Istituto Italiano di Tecnologia, Via Morego 30, 16163, Genova, Italy. {name.surname}@iit.it.

The research leading to these results has received funding from the European Communitys Seventh Framework Programme (FP7/2007-2013) under grant agreement n. 231500/ROBOSKIN.

feedforward force control law and we derive the equations relating the error in the estimation of the contact point with the errors in the contact force and the joint accelerations. Then, in section II-B, we consider a proportional feedback force control law and we repeat the same analysis. Finally, we extend our analysis to a complex real world case, where most of the assumptions that we make in the analytical derivation do not hold. In section II-C we describe a parallel control law that is used to carry out an empirical analysis on the iCub humanoid robot. The robotic platform is described in section III. Section IV reports the results of the tests, both in simulation and on the real robot. The importance of tactile sensing is confirmed by both our analytical analysis and our empirical results, which demonstrate a clear improvement in force and position errors. Finally section V discusses the results of the tests and future work.

II. Contact Force Control

A. Feedforward Force Control with Contact Point Estimation Error

In this section we compute the error in the wrench that is controlled at the contact point, resulting from an error in the estimation of the position of the contact point. Consider the equation of motion of a manipulator in contact with the environment [11]:

$$A(q)\ddot{q} + h(q,\dot{q}) + J_c(q)^T w = \tau, \tag{1}$$

where $q \in \mathbb{R}^n$ is the vector of joint coordinates, $\tau \in \mathbb{R}^n$ is the vector of joint torques, $A(q) \in \mathbb{R}^{n\times n}$ is the joint space inertia matrix, $h(q,\dot{q}) \in \mathbb{R}^n$ is the vector containing all the non-linear terms (e.g. Coriolis, centrifugal and gravity terms), $J_c(q) \in \mathbb{R}^{6\times n}$ is the jacobian of the contact point and $w^T = \begin{bmatrix} f^T & \mu^T \end{bmatrix} \in \mathbb{R}^6$ is the contact wrench vector. In the following, dependency upon q and $\dot{q}$ is no longer denoted to simplify notation. We assume that the manipulator is in rigid contact with the environment and that there are k constrained directions (i.e. $rank(J_c) = k$), hence:

$$\begin{aligned} J_c\dot{q} &= 0 \\ J_c\ddot{q} + \dot{J}_c\dot{q} &= 0 \end{aligned}$$

Under these assumptions, the contact wrench w can be computed as [12]:

$$\begin{aligned} w &= (J_c A^{-1} J_c^T)^{-1}(J_c A^{-1}(\tau - h) + \dot{J}_c\dot{q}) \\ &= \Lambda_c(J_c A^{-1}(\tau - h) + \dot{J}_c\dot{q}), \end{aligned} \tag{2}$$

where we defined the constraint space inertia matrix as $\Lambda_c = (J_c A^{-1} J_c^T)^{-1}$. Consider a simple feedforward force control law:

$$\tau = J^T w_d + \tilde{h} - J_c^T \tilde{\Lambda}_c \dot{J}_c\dot{q}, \tag{3}$$

where $w_d^T = \begin{bmatrix} f_d^T & \mu_d^T \end{bmatrix} \in \mathbb{R}^6$ is the desired contact wrench, $\tilde{h}$ and $\tilde{\Lambda}_c$ are the estimates of h and Λ_c, and $J \in \mathbb{R}^{6\times n}$ is another jacobian of the contact point that considers also the non-constrained directions. Assuming perfect modeling of the dynamic parameters (i.e. $\tilde{h} = h$, $\tilde{\Lambda}_c = \Lambda_c$,) and assuming that the contact geometry allows the manipulator to exert wrench in the desired direction (i.e. $J^T w_d = J_c^T w_d$), this control law results in $w = w_d$ (it is easy to prove it by substituting (3) into (2)).

In order to simplify the analysis, in the following we will assume that the manipulator moves slowly, so that $\dot{J}_c\dot{q} \approx 0$. This assumption is reasonable if we add a damping term to our control law, which then becomes:

$$\tau = J^T w_d + \tilde{h} - k_d\dot{q}, \tag{4}$$

where $k_d > 0$ is a scalar gain. Suppose now that there is an error $e_p \in \mathbb{R}^3$ in the estimate of the contact position and an error $e_o \in \mathbb{R}^3$ in the estimate of the contact orientation:

$$\bar{p} = p + \begin{bmatrix} e_p \\ e_o \end{bmatrix},$$

where $p \in \mathbb{R}^6$ is the real contact point and $\bar{p} \in \mathbb{R}^6$ is the estimated contact point. Assuming that p and $\bar{p}$ are on the same link, their jacobians are related by this equation:

$$\bar{J} = \begin{bmatrix} I_{3\times3} & -[e_p\times] \\ 0_{3\times3} & I_{3\times3} \end{bmatrix} J = S(e_p)J,$$

where $[e_p\times] \in \mathbb{R}^{3\times3}$ is the cross product matrix parametrized by the vector e_p. The torques computed by the control law (4) are:

$$\begin{aligned} \bar{\tau} &= \bar{J}^T w_d + \tilde{h} - k_d\dot{q} \\ &= J^T S(e_p)^T w_d + \tilde{h} - k_d\dot{q} \\ &= J^T(w_d + \begin{bmatrix} 0_3 \\ e_p \times f_d \end{bmatrix}) + \tilde{h} - k_d\dot{q} \\ &= J^T w_d + J_a^T e_p \times f_d + \tilde{h} - k_d\dot{q} \end{aligned} \tag{5}$$

where $J_a \in \mathbb{R}^{3\times n}$ is the angular part of the contact point jacobian $J^T = \begin{bmatrix} J_l^T & J_a^T \end{bmatrix}$. Substituting (5) into (2) we can compute the contact wrench at steady-state (i.e. when $\dot{q} = 0$):

$$\begin{aligned} w &= \Lambda_c J_c A^{-1}(J^T w_d + J_a^T e_p \times f_d + \tilde{h} - h) \\ &= w_d + \Lambda_c J_c A^{-1} J_a^T e_p \times f_d \\ &= w_d + J_c^{T+} J_a^T e_p \times f_d = w_d + e_{wff} \end{aligned} \tag{6}$$

where $J_c^{T+} = \Lambda_c J_c A^{-1}$ is the dynamically-consistent pseudo-inverse of J_c^T [2]. Substituting (6) and (5) into (1) we can compute the joint accelerations:

$$\ddot{q} = A^{-1}(\tau - J_c^T w - h) = A^{-1}(I - J_c^T J_c^{T+}) J_a^T e_p \times f_d \tag{7}$$

Eq. (6) and (7) clearly express the relationship between the contact point estimation error, e_p, and the errors resulting from the control law (3). These equations are quite complex, but we can note that:

1) both e_{wff} and $\ddot{q}$ contain the term $J_a^T e_p \times f_d$, which is the error induced by e_p in the commanded torques
2) the part of $J_a^T e_p \times f_d$ that is selected by J_c^{T+} affects the contact wrench, whereas the remaining part, selected by the null space projection matrix of J_c, generates joint accelerations
3) both e_{wff} and $\ddot{q}$ depend on the desired force f_d, but they are independent of the desired moment μ_d (this makes sense since the relationship between the contact

moment and the joint torques does not depend on the contact point);

4) if the desired force f_d is parallel to the contact point estimation error e_p then both e_{wff} and $\ddot{q}$ are zero;
5) in case we cannot have a precise estimate of the contact point, but we can set an upper bound on $||e_p||$, then it is possible to compute an upper bound of $||e_{wff}||$ and $||\ddot{q}||$ as a function of the maximum norm of f_d and the norm of the dynamically-consistent pseudo-inverse of the contact point jacobian (which depends on the robot kinematics and dynamics parameters).

B. Feedback Force Control with Contact Point Estimation Error

In this section we add a proportional feedback to the control law that we considered in the previous section and we repeat the analysis of the error. The feedback control law is:

$$\tau = J^T(w_d - k_p(w - w_d)) + \tilde{h} - k_d\dot{q}, \tag{8}$$

where $k_p > 0$ is a scalar proportional gain. Suppose, as before, that there is an error e_p in the estimate of the contact point. Besides affecting the jacobian of the contact point, e_p may induce an error in the wrench feedback too. In particular, since we measure the contact wrench using a 6-axis F/T sensor (we follow the procedure described in [13]), then this error can be expressed as:

$$\bar{w} = w - \begin{bmatrix} 0_3 \\ e_p \times f \end{bmatrix} = w - e_w$$

We can compute the commanded torques:

$$\begin{aligned} \bar{\tau} &= \bar{J}^T(w_d - k_p(\bar{w} - w_d)) + \tilde{h} - k_d\dot{q} \\ &= J^T S(e_p)^T(w_d - k_p(w - e_w - w_d)) + \tilde{h} - k_d\dot{q} \\ &= J^T(w_d + e_{w_d} - k_p(w - w_d - e_{w_d})) + \tilde{h} - k_d\dot{q} \\ &= (1 + k_p)J^T(w_d + e_{w_d}) - k_p J^T w + \tilde{h} - k_d\dot{q} \end{aligned}$$

where $e_{w_d}^T = \begin{bmatrix} 0_3^T & (e_p \times f_d)^T \end{bmatrix}$. As before, we can compute the contact wrench at steady-state using (2):

$$\begin{aligned} w = \Lambda_c J_c A^{-1}((1 + k_p)J^T(w_d + e_{w_d}) - k_p J^T w) \\ (1 + k_p)w = (1 + k_p)J_c^{T+}J^T(w_d + e_{w_d}) \\ w = w_d + J_c^{T+}J^T e_{w_d} \\ w = w_d + J_c^{T+}J_a^T e_p \times f_d, \end{aligned} \tag{9}$$

which is equal to the wrench we obtained with the feedforward control law, that is (6). Note that in (9) we used the fact that $J^T w_d = J_c^T w_d$ and $J^T w = J_c^T w$. The first is the same assumption that we made in the previous section, whereas the second is always true since, by definition, wrench can be applied in the constrained directions only. Interestingly, the wrench does not depend on k_p and the introduction of the feedback term does not help to decrease the error. This is sensible considering that e_p induces an error in the wrench measure that is used as feedback. The joint accelerations can be computed as before:

$$\ddot{q} = (1 + k_p)A^{-1}N_c^T J_a^T e_p \times f_d,$$

which are the same as in the feedforward control law, but multiplied by $(1 + k_p)$.

It is interesting to analyze the case where only force is controlled:

$$\begin{aligned} \bar{\tau} &= \bar{J}_l^T(f_d - k_p(f - f_d)) + \tilde{h} - k_d\dot{q} \\ &= (J_l^T + J_a^T[e_p\times])(f_d - k_p(f - f_d)) + \tilde{h} - k_d\dot{q} \\ &= (1 + k_p)\bar{J}_l^T f_d - k_p\bar{J}_l^T f + \tilde{h} - k_d\dot{q}, \end{aligned}$$

where $J_l \in \mathbb{R}^{3\times n}$ is the linear part of the jacobian. Substituting this into (2):

$$\begin{aligned} w = J_c^{T+}((1 + k_p)\bar{J}_l^T f_d - k_p\bar{J}_l^T f) \\ w + k_p J_c^{T+}\bar{J}_l^T f = (1 + k_p)J_c^{T+}\bar{J}_l^T f_d \\ \frac{1}{1 + k_p}w + \frac{k_p}{1 + k_p}J_c^{T+}\bar{J}_l^T f = J_c^{T+}\bar{J}_l^T f_d \end{aligned}$$

As k_p goes to infinity, this equation goes to:

$$J_c^{T+}\bar{J}_l^T f = J_c^{T+}\bar{J}_l^T f_d$$

If $J_c^{T+}\bar{J}_l^T$ is not singular, this implies $f = f_d$. Differently from the previous case, the introduction of a feedback term helps to reduce the error. This is due to the fact that the measured force is not corrupted by the error in the estimation of the contact point, while the moment is.

C. Parallel Force/Position Control

In real world applications most of the assumptions that we made in the previous derivation do not hold: i) contacts are not perfectly rigid, ii) the dynamic parameters of the robot are not perfectly estimated, iii) the contact geometry may not allow the manipulator to apply force in the desired direction. Moreover, robots rarely have to control contact forces only, but they are typically concerned with both position and force at the same time. To investigate the role of precise contact point estimation in a real complex scenario we take a practical approach. In this section we present a parallel control law that will be used on a real robot to see how performances degrade as we introduce errors in the contact point estimation.

The target task is to make the robot slide against an irregular unknown object applying a controlled force and moving the end-effector along a desired path. Given the uncertainties in the environment geometry, the specified path is almost surely incompatible with the desired intensity of the contact force, so the control law has to balance position errors and force errors. We start with one of the parallel control laws presented in [4], that is the superposition of a PD position controller and a PI force controller:

$$\begin{aligned} \tau &= J^T(F - f_d) - k_d\dot{q} + h \\ F &= k_p(x_d - x) - k_f(f_d - f) - k_i\int_0^T (f_d - f)dt \end{aligned}$$

where we simply replaced the cartesian velocity term with a joint velocity term. The integral term in the force controller ensures dominance of the force loop over the position loop. We need to modify this control law because, differently from [4], the interested position and force are relative to two

distinct points: the end-effector x and the contact point c. The modified control law is:

$$\begin{aligned} \tau &= J_c^T(F_c - f_d) + J^T F_p - k_d\dot{q} + h \\ F_p &= k_p(x_d - x) \\ F_c &= -k_f(f_d - f) - k_i \int_0^T (f_d - f)dt \end{aligned} \tag{10}$$

where J and J_c are respectively the jacobian of the end-effector and the jacobian of the contact point. Since we are not concerned with the force direction, but just with its norm, we decided to use the direction of the measured force as desired direction:

$$f_d = \frac{f}{||f||} f_N, \quad if \quad ||f|| > \frac{||f_d||}{2}$$

where f_N is the desired force norm. In the approaching phase, when the norm of the measured force is less than half of the desired norm force, a predefined force direction is used. We assume that the robot has a rough estimate of the position of the object and so it can define an initial force direction. However, given the irregularities in the environment surface, the direction of the initial desired force may be inadequate (e.g. it may not be possible to apply a vertical force on a 45°inclined plane). Adapting the direction of f_d helps to compensate for the lack of knowledge about the geometry of the environment and it makes the controller more robust to errors in the initial direction of f_d.

III. Test Platform

The proposed controllers have been tested on the humanoid robot iCub. The iCub is an open robotic platform, aimed at the study of embodied cognition [14]. Its high number of degrees of freedom (53 in total, 30 in the upper body of which 9 just in each hand) and its small height of 104 cm, distinguish this robot from the other humanoid platforms worldwide. A large variety of sensors are mounted on the robot: digital cameras, gyroscopes and accelerometers, microphones, force/torque sensors and a distributed sensorized skin.

A. The force/torque sensor

The iCub is equipped with four custom made F/T sensors [13], each one located in each limb. The location of the sensors differs from the usual distal configuration at the end-effector. Indeed they are located in between the shoulder and the elbow in the arm, and in between the knee and the hip in the legs. The solution allows the measurement of both internal dynamics and external forces exerted on the whole limb, in contrast with the distal configuration, whose measurements would be limited to the end-effector.

B. The robot skin

A compliant skin[15] incorporating a distributed pressure sensor, based on capacitive technology, is currently mounted on the torso, arms, palms and fingertips of the iCub (see Fig. 1). The skin is organized in triangular modules, except for the fingertips, where a particular solution has been designed for complying with the small size and round shape. Each module, composed by 12 taxels (see Figure 2), is able to scan locally 12 measurements of capacitance and send them through a serial bus.

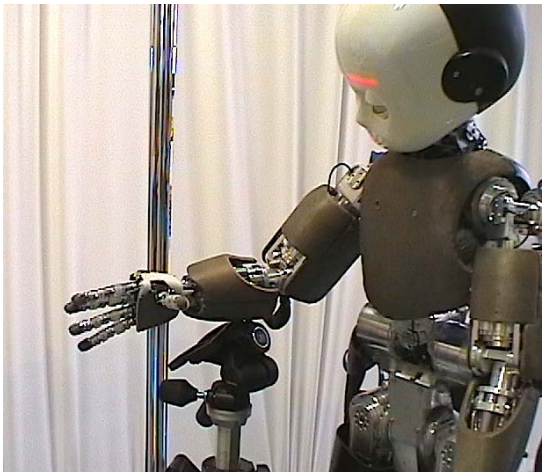

Fig. 1. The iCub robot, with skin mounted on the torso, arms, palms and fingertips. The iCub is sliding its forearm agains the top of the tripod that is standing in front of it.

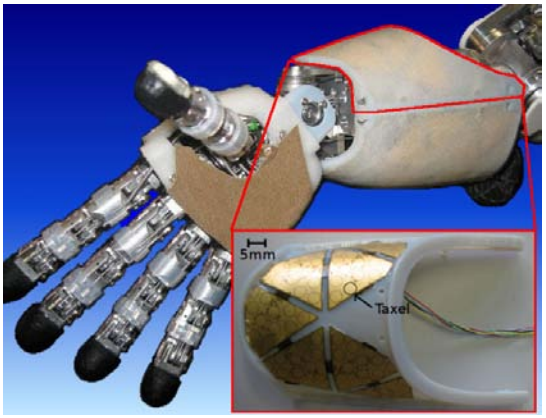

Fig. 2. Right arm of the iCub robot, with skin mounted on the forearm (not covered with the lycra yet), palm and fingertips. In the red box, a detailed view of the forearm cover and the placement of the sensors [15]. This part is not covered with the silicone foam yet.

The basis of the sensor is a flexible printed circuit board (PCB). A 2/3 mm thick layer of silicone foam is placed above the PCB, covering the 12 taxels. The role of this layer is two-fold: (i) it acts as a deformable dielectric for the capacitive pressure sensor and (ii) it makes the skin compliant. A second conductive layer of lycra is placed on top of the silicon foam, in order to make the sensors sensitive to every material, regardless of its electrical properties. In every skin triangle the 12 taxels can be read either independently at 50 Hz, or as an average of them at about 500 Hz.

C. Software

The software library *iDyn* [16] is at the core of the implementation of force control on the iCub. Using the dynamic parameters of the robot (extracted from the CAD

model) and the data of F/T sensors and tactile sensors, *iDyn* can:

- estimate the joint torques to simulate joint torque sensors and so implement joint torque control in the control boards of the motors;
- estimate the contact forces [17].

The information relative to the contact points comes from a software module called *SkinManager*, which uses the 3D positions of the tactile sensors to compute the center of pressure of each contact area. To obtain this information the tactile sensors were previously calibrated using the technique presented in [18].

IV. Experimental Results

As already mentioned in section II-C, most of the simplifying assumptions that we made in our derivation do not hold on a real robot. Furthermore, we have to take into account that: i) measurements of contact forces are usually noisy and they may be affected by the errors in the dynamic parameters of the robot, ii) the quality of the tracking of the torque controllers may be poor. All these factors make the validation on the robot of the presented analysis extremely difficult. Hence we decided to use a simulated robot to validate the analytical analysis and to carry out additional tests on the real robot as an empirical analysis of more complex scenarios.

A. Simulation Tests

We use a simulated puma560 robot arm with 6 dofs, which is provided with the matlab robotics toolbox [19]. Both the motors and the force/torque sensor are simulated as low-pass filters with cut frequency of 40 Hz and 20 Hz, respectively. In the simulation the manipulator is in rigid contact with the environment at the end-effector. An error in the estimation of the contact location $e_p = [0.1; 0; 0]m$ is introduced and we command a desired force $f_d = [0; 10; 0]N$ and a desired moment $\mu_d = [0; 0; 1]Nm$. The four tests span two different constraint situations and two control laws. In the tests IV-A.1 and IV-A.3 we assume that the end-effector of the robot is completely constrained (i.e. $rank(J_c) = 6$), so it can apply force and moment in all directions, but it cannot move. In the tests IV-A.2 and IV-A.4 we assume that the end-effector can only exert forces on the environment (i.e. $rank(J_c) = 3$), so it cannot apply moment, but it can move. The first two tests use the feedforward control law (3), whereas the last two tests use the feedback control law (8).

1) Feedforward Wrench Control: As predicted by (6) and (7), the error in the commanded torques is totally projected in the contact wrench, in particular it affects the contact moment only, resulting in $f = [0; 10; 0]$ and $\mu = [0; 0; 2]$. The desired contact force is correctly applied and the joint accelerations are zero, because the contact jacobian J_c has zero nullspace.

2) Feedforward Force Control: In this case the contact jacobian J_c has a non-trivial nullspace, so a part of the error in the commanded torques is selected by J_c^{T+} and it affects the contact force, resulting in $f = [0; 11.66; 0]N$. The remaining part, which is selected by the null space projection matrix of J_c, generates joint accelerations, resulting in $||\ddot{q}|| = 3.67m/s^2$.

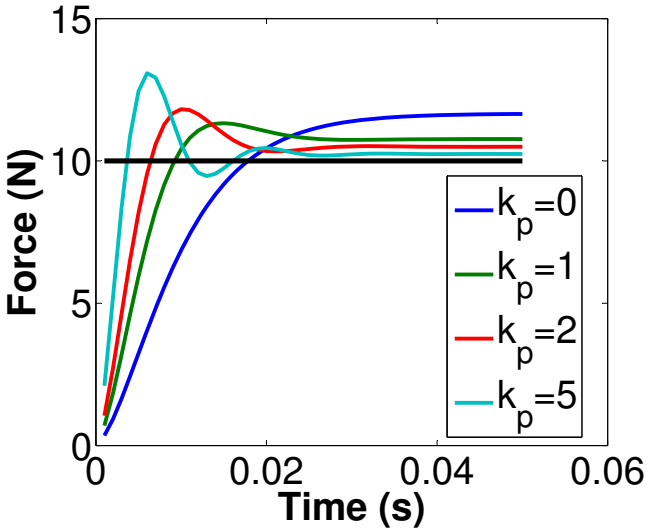

Fig. 3. Contact force with proportional feedback force control for different values of the proportional gain k_p.

3) Feedback Wrench Control: As predicted by (9) the result is the same as in the feedforward case: the error affects the contact moment only and it is independent of the proportional gain k_p. Joint accelerations are zero.

4) Feedback Force Control: Similarly to test IV-A.2, the contact localization error affects both the contact force and the joint accelerations. Since the force feedback is not affected by e_p, it helps to reduce both errors. Fig. 3 shows how the steady-state error of the contact force decreases as k_p increases. Of course as k_p goes up the overshoot of the system rises. The joint accelerations decrease as k_p increases.

B. Robot Tests

In these tests we control three joints of the robot's arm: the elbow joint and two out of the three shoulder joints.

1) Feedforward Force Control: The first test uses the control law (3). The right forearm of the robot lies on a rope, which is fixed to a rigid structure located above the robot. In this configuration the robot is able to apply downward forces on the rope. A downward force of 5 N is commanded. When the tactile sensors are not used, the contact point is assumed to be at the end-effector, which is about 9 cm off the real contact point. Without using the tactile sensors we found a norm of the force error of ~ 4 N, whereas when using the tactile sensors the error norm decreases to ~ 1.7 N.

2) Parallel Control: This test uses the parallel control law (10) with $k_p = 150$, $k_d = 0.02$, $k_f = 0.5$ and $k_i = 0.02$. The robot starts with the lower part of its forearm in contact with an irregular rigid object, i.e. a tripod for cameras (see Fig. 1). The desired trajectory of the end-effector spans only the x direction, moving 5 cm back and 5 cm forth in a straight line. One whole cycle lasts about 33 seconds (the movement is quite slow). While moving the end-effector, the robot tries to maintain a contact force of 3 N, regardless

of the force direction. The performance benefits from the precise estimation of the contact point: when using the tactile sensors the mean norm of the force error decreases from ~ 1.4 N to ~ 1.1 N, and the mean norm of the position error decreases from ~ 2.3 cm to ~ 1.5 cm. The force error does not converge to a stable value despite the integral term in the control law. This is due to the fact that the integral is reset every time the reference position is modified (i.e. about every 16 seconds). As expected, the improvements due to a precise estimate of the contact point are not as large as in the previous test, because, as proved is section II-B, the feedback helps to reduce the force error.

V. Conclusions And Future Work

In this paper we analyze how knowledge of the location of the contact points affects force control tasks. We show how errors in the estimation of contact points may affect the contact forces and, possibly, the joint accelerations. We show that the introduction of a feedback term may not necessarily help to reduce the errors, if the feedback itself is affected by the estimation error.

Tests on a simulated 6-dof robotic arm validate our hypotheses. Moreover, we present the results of two experiments on the iCub robot. In these tests we cannot use the equations that we found in our analytical analysis because most of the assumptions that we made in the derivation do not hold. However, the presented results are important because they empirically prove the effectiveness of precise contact point estimation, even in complex real-world scenarios. In the first test, using a feedforward force control law we measure a large drop in the force error (from 4 N to 1.7 N) when tactile feedback is used to locate the contact point. Then, in the second test, we use a parallel control law to make the iCub maintain contact with a rigid irregular object, while moving the end-effector along a straight line. Tests with and without the tactile feedback reveal a significant improvement in the performance when using the tactile system. Differently from most works in the literature, we do not use any geometric model of the robot or the environment. The lack of knowledge about the external world is compensated by tactile and force feedback.

We intend to extend the presented analysis to more complex control laws such as impedance control, hybrid control and parallel control. Also, we could investigate the case where contacts are not perfectly rigid.

In the near future we plan to use the presented parallel controller in conjunction with the method for skin spatial calibration presented in [18]. The calibration method infers the positions of the tactile sensors by measuring the interaction forces exchanged between the sensorized part and the environment. In [18], a human operator applied forces on the robot's skin. We are planning to extend this work by programming the robot to make contact with the environment autonomously. Since at the beginning of the calibration the positions of the tactile sensors would be unknown, the analysis presented in this paper provides an estimation of the maximum forces that we can expect to arise during the most critical phases of the calibration.

VI. Acknowledgments

The authors would like to thank Marco Randazzo.

References

[1] N. Hogan, "Impedance control: An approach to manipulation," in *American Control Conference, 1984*. IEEE, 1985, pp. 304–313.

[2] O. Khatib, "A unified approach for motion and force control of robot manipulators: The operational space formulation," *IEEE Journal on Robotics and Automation*, vol. 3, no. 1, pp. 43–53, Feb. 1987.

[3] R. Anderson and M. Spong, "Hybrid impedance control of robotic manipulators," *IEEE Journal on Robotics and Automation*, vol. 4, no. 5, pp. 549–556, 1988.

[4] S. Chiaverini and L. Sciavicco, "The parallel approach to force/position control of robotic manipulators," *IEEE Transactions on Robotics and Automation*, vol. 9, no. 4, pp. 361–373, 1993.

[5] J. Park and O. Khatib, "Contact consistent control framework for humanoid robots," in *Robotics and Automation, 2006. ICRA 2006. Proceedings 2006 IEEE International Conference on*, no. 1. IEEE, 2006, pp. 1963–1969.

[6] L. Righetti, J. Buchli, M. Mistry, and S. Schaal, "Inverse dynamics control of floating-base robots with external constraints: A unified view," *2011 IEEE International Conference on Robotics and Automation*, pp. 1085–1090, May 2011.

[7] L. Sentis, J. Park, and O. Khatib, "Modeling and control of multi-contact centers of pressure and internal forces in humanoid robots," *2009 IEEE/RSJ International Conference on Intelligent Robots and Systems*, pp. 453–460, Oct. 2009.

[8] S. J. Gordon and W. T. Townsend, "Integration of Tactile-Force and Joint -Torque Information in a Whole-Arm Manipulator," in *Robotics and Automation, 1989. Proceedings., 1989 IEEE International Conference on*, 1989, pp. 464–469.

[9] J. Park and O. Khatib, "Multi-link multi-contact force control for manipulators," in *Robotics and Automation, 2005. ICRA 2005. Proceedings of the 2005 IEEE International Conference on*, no. Figure 2. IEEE, 2005, pp. 3613–3618.

[10] A. Jain, M. Killpack, and A. Edsinger, "Manipulation in Clutter with Whole-Arm Tactile Sensing," *Under Review*, pp. 1–20, 2011.

[11] B. Siciliano and O. Khatib, *Springer Handbook of Robotics*, B. Siciliano and O. Khatib, Eds. Springer, 2008, vol. 15, no. 3.

[12] M. Mistry, J. Buchli, and S. Schaal, "Inverse dynamics control of floating base systems using orthogonal decomposition," *2010 IEEE International Conference on Robotics and Automation*, no. 3, pp. 3406–3412, May 2010.

[13] M. Fumagalli, M. Randazzo, F. Nori, L. Natale, G. Metta, and G. Sandini, "Exploiting proximal F/T measurements for the iCub active compliance," in *Intelligent Robots and Systems (IROS), 2010 IEEE/RSJ International Conference on*. IEEE, 2010, pp. 1870–1876.

[14] G. Metta, G. Sandini, D. Vernon, L. Natale, and F. Nori, "The iCub humanoid robot: an open platform for research in embodied cognition," in *Workshop on Performance Metrics for Intelligent Systems, National Institute of Standards and Technology*. Washington DC, USA: ACM, 2008.

[15] A. Schmitz, P. Maiolino, M. Maggiali, L. Natale, G. Cannata, and G. Metta, "Methods and Technologies for the Implementation of Large-Scale Robot Tactile Sensors," *IEEE Transactions on Robotics*, vol. 27, no. 3, pp. 389–400, June 2011.

[16] S. Ivaldi, M. Fumagalli, M. Randazzo, F. Nori, G. Metta, and G. Sandini, "Computing robot internal/external wrenches by means of inertial, tactile and f/t sensors: theory and implementation on the icub," in *Proc. of the 11th IEEE-RAS International Conference on Humanoid Robots, Bled, Slovenia*, 2011.

[17] A. Del Prete, L. Natale, F. Nori, and G. Metta, "Contact Force Estimations Using Tactile Sensors and Force / Torque Sensors," in *Human Robot Interaction 2012*, 2012, pp. 0–2.

[18] A. Del Prete, S. Denei, L. Natale, F. Mastrogiovanni, F. Nori, G. Cannata, and G. Metta, "Skin Spatial Calibration Using Force/Torque Measurements," in *Intelligent Robots and Systems (IROS), 2011 IEEE/RSJ International Conference on*, 2011.

[19] P. Corke, "Robotics, Vision and Control," in *Robotics Vision and Control*. Springer Berlin Heidelberg, 2011, pp. 452–495.